Microchimica Acta (2020) 187:333
https://doi.org/10.1007/s00604-020-04307-6

ORIGINAL PAPER

# A low-field nuclear magnetic resonance DNA-hydrogel nanoprobe for bisphenol A determination in drinking water

Jing-Yi Wang[1,2] · Qi-Yue Guo[2,3] · Zi-Yi Yao[2,3] · Na Yin[1,2] · Shu-Yue Ren[2] · Ye Li[2,3] · Shuang Li[2] · Yuan Peng[2] · Jia-Lei Bai[2] · Bao-An Ning[2] · Jun Liang[1] · Zhi-Xian Gao[2]

Received: 11 December 2019 / Accepted: 29 April 2020


## Abstract

A low-field nuclear magnetic resonance (LF-NMR) DNA-hydrogel (LNDH) nanoprobe was designed for bisphenol A (BPA) determination. It consists of $Fe_3O_4$ superparamagnetic iron oxide nanoparticles (SPIONs) and a DNA-hydrogel technology. $Fe_3O_4$ SPIONs were encapsulated in the DNA-hydrogel to form an aggregated state. After adding BPA, the gel system transformed into a sol gel due to the target-aptamer specific binding. The coated gathered particles dispersed and thus, the relaxation time $T_2$ declined. The LNDH nanoprobe was developed to realize a simple, sensitive, and effective BPA determination method without repeated magnetic separation steps. Under the optimal experimental conditions, the determination range of the LNDH biosensor was $10^{-2}$~$10^{2}$ ng $mL^{-1}$ and the limit of determination was 0.07 ng $mL^{-1}$. The LNDH nanoprobe was applied to two kinds of water samples (tap water and bottled water). The recovery ranged from 87.85 to approximately 97.87%. This strategy offered a new method to detect BPA by LF-NMR. It is also expected to be applicable in related fields of food safety determination, environmental monitoring, and clinical diagnosis.

**Keywords** LF-NMR · DNA-hydrogel · $Fe_3O_4$ SPIONs · BPA

## Introduction

Endocrine-disrupting chemicals (EDCs) have gained increasing attention because of their potential impacts on human health [1]. EDCs can mimic the action of the hormone estrogen disturbing the estrogen-estrogen receptor binding process (hormonal pathways) [2] and causing possible health effects [3]. Bisphenol A (BPA) is a kind of EDCs and is commonly used in our daily household products or various kinds of packaging. It is a major kind of raw materials used to produce polycarbonate plastic, epoxy resin, thermal-resistant products, and health care products [4, 5]. The annual BPA production was estimated to be more than 5 million tons in 2015 [6]. Based on daily use conditions and their potential effects on human health, it is necessary to propose a sensitive, fast, and easy to operate method to detect BPA. Several kinds of effective techniques have been developed for BPA determination. Traditional methods including high-performance liquid chromatography (HPLC) [7, 8], ultraviolet and visible spectrophotometry (UV-Vis), and mass spectrometry (MS) [9] have been widely used. These methods are mature, sensitive, and stable, but these methods also require complicated predisposal processes, professional operators, and/or expensive instruments. The methods are time-consuming, which is also a drawback. Chromatography generally requires expensive apparatuses, large amounts of organic solvents and other chemicals, and extensive sample pretreatment such as purification, concentration, and derivatization. However, it takes only 6 h to synthesize $Fe_3O_4$ superparamagnetic iron oxide nanoparticles (SPIONs) with a simple method. Our method requires only a

**Electronic supplementary material** The online version of this article (https://doi.org/10.1007/s00604-020-04307-6) contains supplementary material, which is available to authorized users.

✉ Jun Liang
jliang1118@yeah.net

✉ Zhi-Xian Gao
gaozhx@163.com

[1] State Key Laboratory of Food Nutrition and Safety, Tianjin University of Science and Technology, Tianjin 300457, China

[2] Tianjin Key Laboratory of Risk Assessment and Control Technology for Environment and Food Safety, Institute of Environmental and Operational Medicine, Tianjin 300050, China

[3] College of Chemistry and Materials Science, Shanghai Normal University, Shanghai 200234, China

small amount of reagent to complete the test and does not require large apparatuses. The low-field nuclear magnetic resonance (LF-NMR) detection method is superior to the traditional chromatography in these points.

Biosensor technology is becoming increasingly attractive in the field of EDC determination. Many types of methods, including electrochemical biosensors [10–14], fluorescence biosensors [1, 4, 15–19], and SERS biosensors [20, 21], have been applied in BPA determination. Magnetic relaxation switching assays with a broad and tunable determination range can greatly improve current magnetic sensors for biochemical determinations [22]. Combining click chemistry with low-field NMR technology develops biosensors with practical determination capabilities [23]. For BPA determination, LF-NMR is a relatively new technology. Its noninvasive and nondestructive nature coupled with its high discriminative power makes it become an invaluable analysis tool for a wide range of applications in many fields [24]. LF-NMR technology refers to the spectroscopy technique based on nuclear relaxation analysis with a field strength below 0.5 Tesla. The longitudinal relaxation time $T_1$ (spin-lattice relaxation), transverse relaxation time $T_2$ (spin-spin relaxation), and the diffusion coefficient can reflect the motion properties of hydrogen protons in a system. The determination of hydrogen proton changes in a system by LF-NMR provides a new method for detecting EDCs. Magnetic separation is a necessary operation step in most LF-NMR studies. This step makes the experimental operation more complicated and results in a lengthier process with some loss of the sample. Combining SPIONs and DNA-hydrogels can effectively compensate for the above deficiencies. A hydrogel is a three-dimensional polymer network, in which the individual hydrophilic polymer chains are connected by the physical or chemical bonds. It has become one of the most appealing polymer materials and is usually used to prepare sustainable-release systems. DNA-hydrogels not only have the good biocompatibility and programmability of DNA but also have the hydrophilic and mechanical properties of hydrogels. This kind of material has excellent performance in pharmaceutical development and regenerative medicine based on the above merits [25, 26]. Herein, we proposed an LF-NMR DNA-hydrogel determination strategy.

In this research, we provide an LNDH nanoprobe method to detect BPA using an aptamer-functional hydrogel system and $Fe_3O_4$ SPIONs. In this design, the introduction of the target molecules destroys the hydrogel system by specific binding between the target and aptamer to release the encapsulated $Fe_3O_4$ SPIONs, which results in changes in the particle state from gathered to scattered. In this way, the $T_2$ relaxation time declines, and the signal change is detected by LF-NMR. The proposed LF-NMR aptamer-functional hydrogel nanoprobe is a promising method for BPA determination.

## Experimental methods

### Materials and instruments

All related materials and instruments are shown in the supplementary material.

### Preparation of the hydrogel

Freshly prepared initiators, including 10 mg APS, 5 μL TEMED, and 95 μL deionized water, were used. Acrydite-modified S-A and S-B were centrifuged for 30 s and diluted to 5 μmol $L^{-1}$ with deionized water. Then, the above solutions were diluted to 2.5 μmol $L^{-1}$ with 1.5% acrylamide solution, after vacuum desiccation for 3 min to remove oxygen at room temperature. The above initiator was added according to a specific ratio and vacuum-desiccated for 5 min to remove oxygen at room temperature. Then, the two tubes were shaken overnight to form polymer strands A (PS-A) and B (PS-B). Linker-Apt was centrifuged for 30 s and diluted to 2.5 μmol $L^{-1}$ with deionized water. Then, the samples were denaturized at 95 °C and slowly cooled down to room temperature to ensure the formation of complete and stable structures.

PS-A, PS-B, and Linker-Apt were mixed in a stoichiometric ratio (1:1:1), and $Fe_3O_4$ SPIONs were added to the above DNA-hydrogel system. The mixture was shaken at 37 °C for 2 h (1000 rpm) to form the hydrogel system. Then, the samples were stored at 4 °C to preserve them.

### The determination process of the proposed strategy

For BPA determination, methanol was used to prepare a BPA solution at a concentration of 1 mg $mL^{-1}$. Then, 10 μL of the prepared BPA solution was added to 90 μL of PBS. In this way, the solution was diluted ten times to 1 pg $mL^{-1}$. Different concentrations from 1 mg $mL^{-1}$ to 1 pg $mL^{-1}$ of BPA solution were added into the determination system respectively. When mixed totally, the above mixture was shaken and incubated at 37 °C for 2 h (1000 rpm). Then, the centrifuge tubes were removed without repeated magnetic separation operations, and the $T_2$ relaxation time was tested by LF-NMR directly.

The DNA-hydrogel was characterized by SEM under the condition of gold plating on the silicon surface. The LSCM images also displayed that the DNA-hydrogel was formed and the SPION-labeled fluorescent probe was encapsulated.

Four different concentrations (1~1000 ng $mL^{-1}$) of BPA solution were chosen and added to four different centrifuge tubes with the same determination system. When mixed completely, the above mixture was shaken and incubated at 37 °C for 2 h (1000 rpm). Then, the centrifuge tubes were removed and 50 μL was drawn for characterization by DLS.

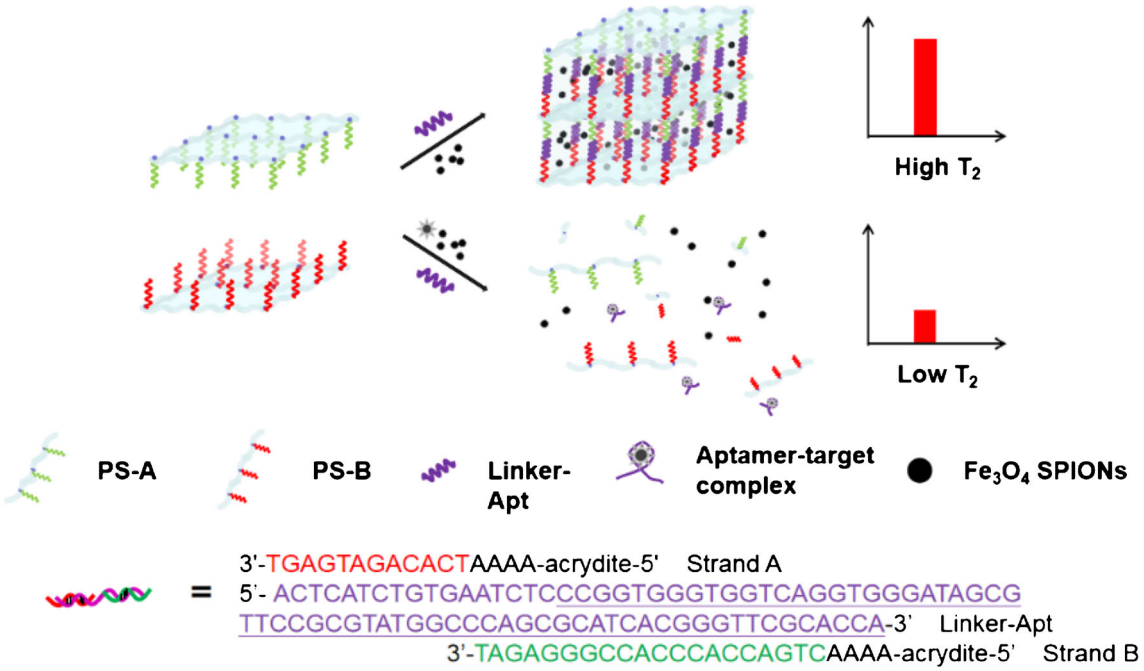


**Scheme 1** Schematic of the LNDH biosensor. Acrydite-modified single-strand DNA was copolymerized with acrylamide to form linear DNA–polyacrylamide conjugates PS-A/B, and the aptamer and $Fe_3O_4$ SPIONs were added to form DNA-hydrogels. When the aptamer captured the target, the hydrogel was destroyed to disperse the coated $Fe_3O_4$ SPIONs. $T_2$ relaxation time declined

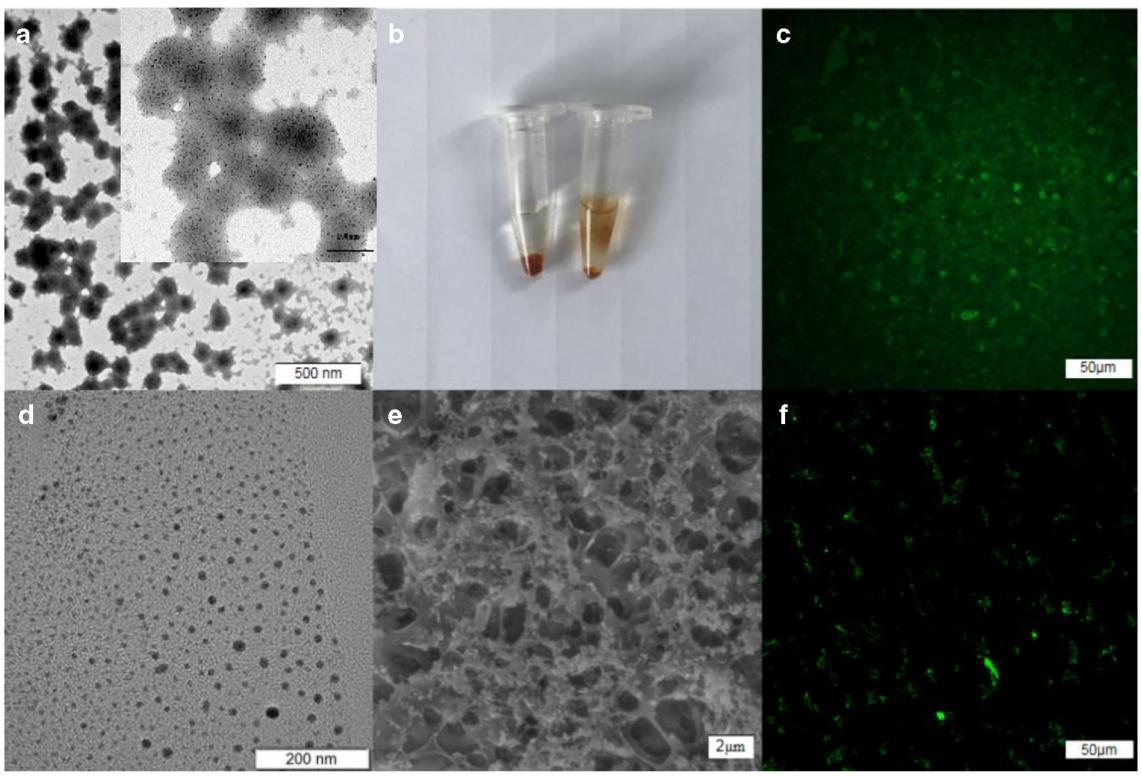


**Fig. 1** Characterization of the LNDH before and after adding BPA. **a**, **d** TEM images of the LNDH biosensor before and after adding BPA. **b** The image of the determination system visual change. **c**, **f** LSCM images of the LNDH biosensor before and after adding BPA. **e** SEM images of the LNDH biosensor

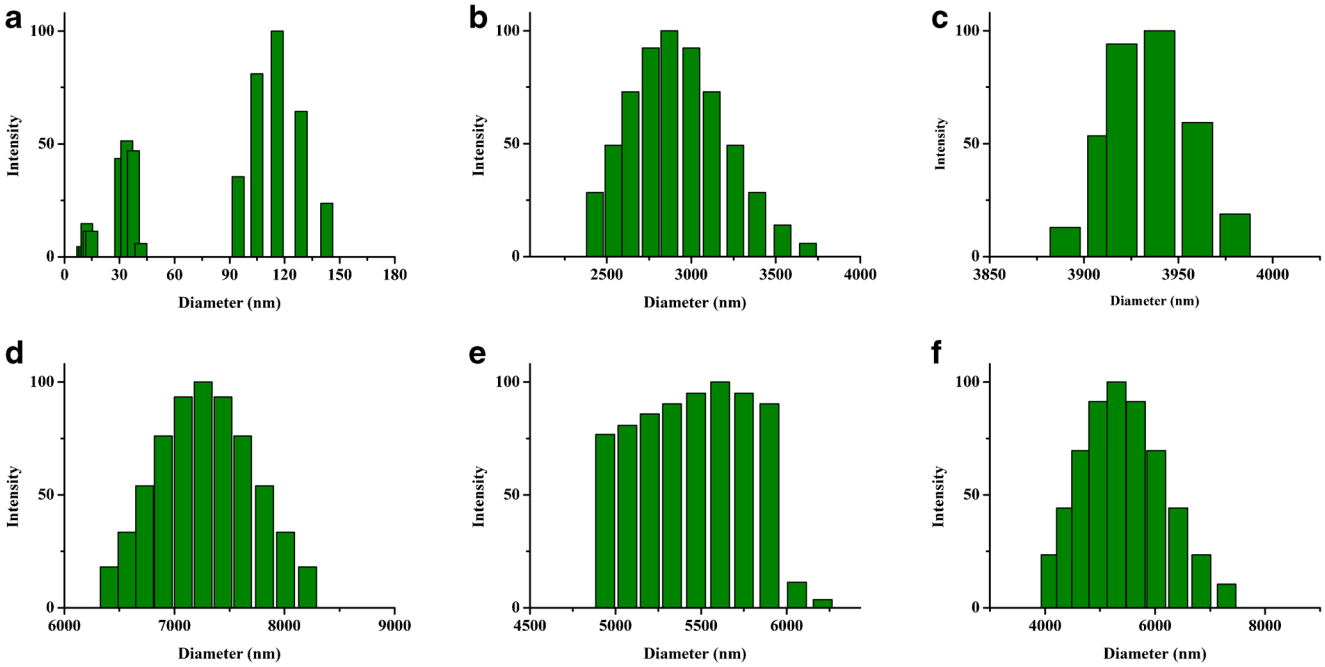


**Fig. 2** DLS images of LNDH biosensors with different concentrations of BPA. **a**, **f** The size distribution of LNDH before and after forming a hydrogel. **b**–**e** The size distribution of different concentrations of BPA (100, 10, 1, 0.1, and 0 ng $mL^{-1}$)

## Selectivity

To investigate the selectivity of this strategy, we chose five BPA chemical mimics including BPB, BPC, BP, 6F-BPA, and tb-BPA (these chemicals are very similar in structure with BPA because they all contain two benzene rings) to conduct the next process. These chemical mimics (10 μg $mL^{-1}$) were separately added to the tubes and their $T_2$ relaxation time was recorded by LF-NMR.

## Real sample analysis

To investigate the practicability of real sample analysis, we challenged our method with tap water and bottled water that could be contaminated by BPA. Several environmental water samples spiked with BPA at concentrations of $10^5$, $10^3$, and 10 ng $mL^{-1}$ were tested using the proposed method. The tap water was filtered using a needle-type filter to remove the particulate in advance. A BPA solution was prepared at a concentration of 1 mg $mL^{-1}$ with methanol, and then, diluted to $10^5$, $10^3$, and 10 ng $mL^{-1}$ with the tap water or the bottled water separately. Three parallel samples were set up for the different types of water.

# Results and discussion

## Working principle of the proposed nanoprobe

An LNDH nanoprobe for sensitively detecting BPA was proposed. The synthesis process and determination principle of

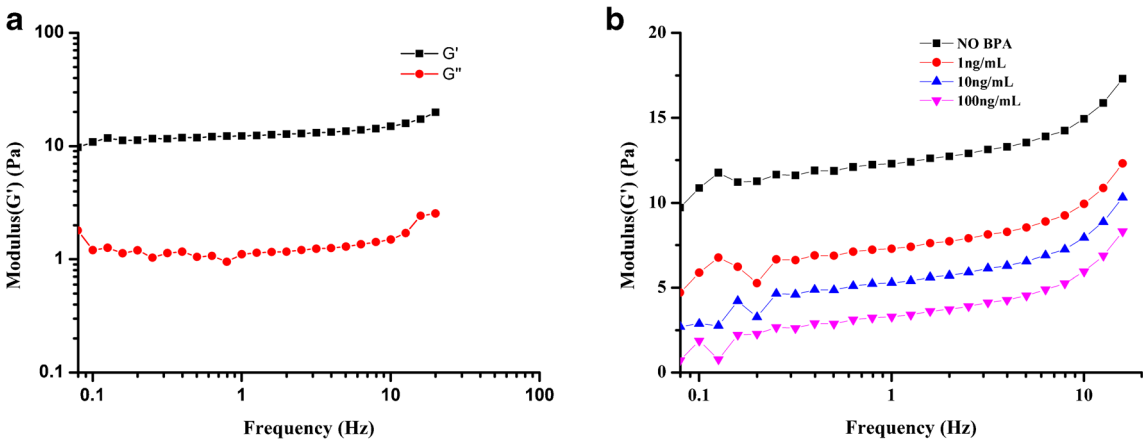


**Fig. 3** Dynamic rheology behaviors of LNDH biosensor. **a** The storage modulus (G′) and loss modulus (G″) curves of LF-NMR DNA-hydrogel biosensor. **b** The complex viscosity of the determination system with different concentrations of BPA

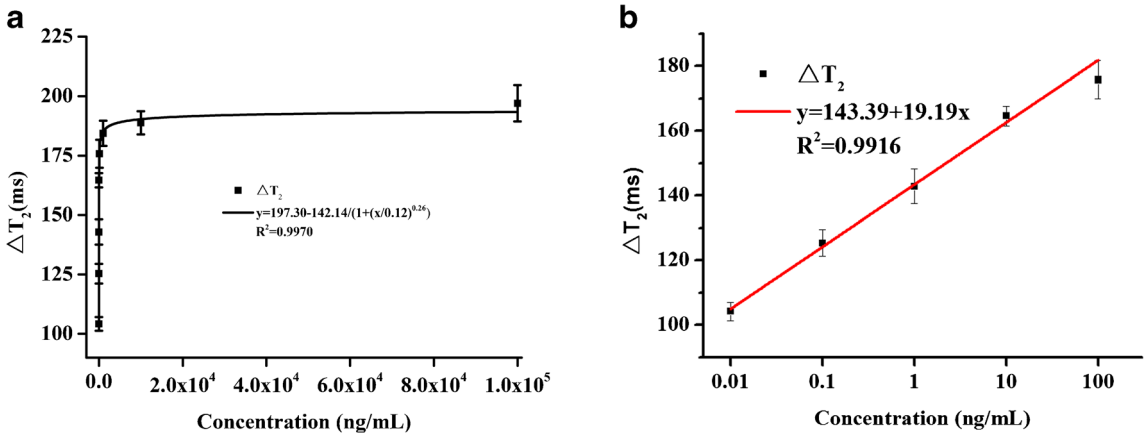


**Fig. 4** **a** Relaxation time $\Delta T_2$ corresponding to different concentrations of BPA: $10^{-2}$~$10^{5}$ ng $mL^{-1}$. **b** The image shows the linear relationship between the BPA concentrations of $10^{-2}$~$10^{2}$ ng·$mL^{-1}$

the strategy are shown in Scheme 1. First, two types of acrydite-modified single-strand DNA (S-A and S-B) were copolymerized with acrylamide to form linear DNA–polyacrylamide conjugates, named PS-A or PS-B. When mixed in the same amounts, the grafted polymers are in a transparent liquid state. Then, adding $Fe_3O_4$ SPIONs into the mixture, the hydrogel formed a three-strand structure after the addition of the initiator BPA aptamer. In the hybridization process, the cross-linking ratio of polyacrylamide increased which resulted in the increased viscosity of the polymer solution. When adding the target BPA, the aptamer captures the target molecule which resulted in destroying the hydrogel structure. The coated SPIONs return to a dispersed state, and $T_2$ therefore decreases (parameters: Q-CPMG TW (ms) 8000 TE:0.8 NECH:17,000).

## Characterization of the LF-NMR DNA-hydrogel nanoprobe

The TEM image clearly indicates that the SPIONs were encapsulated in the hydrogel in Fig. 1a. The diameter of the SPIONs was approximately 15~20 nm, and the particles were aggregated in the hydrogel and distributed evenly. Figure 1d shows the change after adding BPA. Figure 1d clearly shows that the particle state changed from aggregation to dispersion. The DNA-hydrogel was characterized by SEM under the condition of gold plating on the silicon surface. As shown in Fig. 1e, the DNA-hydrogel structure was clearly porous. The pore size was less than 1 μm in diameter. Figure 1b revealed the visual differences in the hydrogel states before and after adding BPA. The LSCM images also displayed that the DNA-hydrogel was formed and the fluorescent probe-labeled SPIONs were encapsulated in Fig. 1c. As shown in this figure, the fluorescence intensity was weak due to agglomeration of the magnetic nanoparticles, but after adding the target, as Fig.1f displays, the magnetic nanoparticles diffused into the system, which results in recovery of the fluorescence intensity and dispersion.

As shown in Fig. 2, the DLS images revealed the size distribution of the $Fe_3O_4$ SPIONs, in an aptamer-functional hydrogel system with different concentrations of BPA (100, 10, 1, 0.1, and 0 ng $mL^{-1}$). In Fig. 2a, the size distribution of $Fe_3O_4$ SPIONs was almost 100 nm and mostly concentrated at 30~45 nm. When forming the hydrogel system, the size increased to approximately 8 μm, as shown in Fig. 2f. However, after adding four different concentrations of BPA, the size distribution declined with increasing concentration, as shown in Fig. 2b–e.

The viscoelastic properties of the proposed method were examined by rheological testing. The storage modulus (G′) and loss modulus (G″) are used to evaluate the ability of a

**Table 1** Comparison of our developed method with the existing methods for detecting BPA

| Methods | Applied materials | LOD | Determination range | Ref. |
|---|---|---|---|---|
| Electrochemical | MIP and AuNPs | 2.56 ng $mL^{-1}$ | 2.28~11.4 ng $mL^{-1}$ | [27] |
| Electrochemical | AuPd and carbon nanotubes | 13.698 pg $mL^{-1}$ | 41.094–4109.4 mg $mL^{-1}$ | [28] |
| SERS | SERS-improved LFA | 0.073 ng·$mL^{-1}$ | 0.01~100,000 ng $mL^{-1}$ | [29] |
| Fluorescence | FAM-Apt and MNPs | 0.047 ng $mL^{-1}$ | 0.20~8.00 ng $mL^{-1}$ | [1] |
| LF-NMR | SPIONs and DNA-hydrogel | 0.07 ng $mL^{-1}$ | 0.01~100 ng $mL^{-1}$ | This Work |

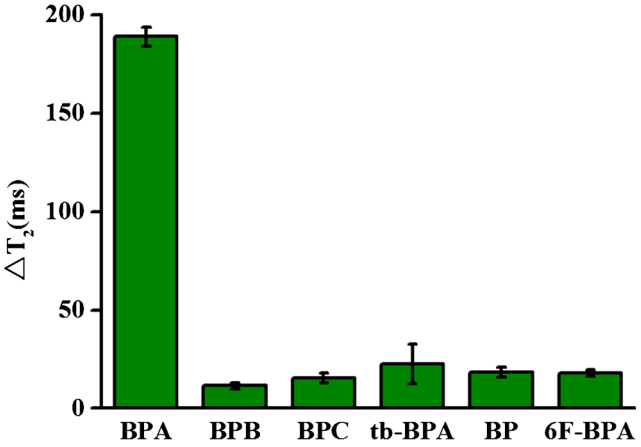


**Fig. 5** Selectivity of the aptamer-functional DNA-hydrogel system toward BPA ($10^4$ ng $mL^{-1}$) against other structural analogs (BPB, BPC, Tb-BPA, BP, and 6F-BPA). Error bars were obtained from three experiments

deformed material to restore to its original geometry and the propensity of material flow propensity. The results are shown in Fig. 3.

As shown in Fig. 3a, the modulus (G′ and G″) revealed the slight frequency dependence over the entire tested frequency range. G′ was approximately 1 order of magnitude higher than G″, and the values did not cross over each other during the entire test range, which implied that the elastic response is predominant and that the material had a permanent network with high degree of cross-linking. G″ was always lower than G′, which suggested the gel-like behavior of the system. Figure 3b shows that the storage modulus (G′) of hydrogels with different concentrations of BPA was lower than that of the control group without BPA, which implied that BPA was harmful to gelation and further improved the mechanical strength of the resulting hydrogels.

## Optimization of the experimental conditions

In the proposed strategy, the concentrations of S-A/B and the $Fe_3O_4$ SPIONs and the reaction temperature played important roles in the whole process. Usually, the stability of a hydrogel is affected by the reaction temperature. The change in relaxation time $T_2$ was recorded as the temperature increased. As shown in Fig. S1, the signal changed apparently at different temperatures. The graph clearly shows that 37 °C is the optimal experimental temperature.

The signal change increased as the reaction temperature ranged from 4 to 37 °C and then decreased over 37 °C. These phenomena can be interpreted that DNA reaction is relatively stable at 37 °C. To facilitate the experiment, 37 °C was selected as the optimal reaction temperature.

Furthermore, the effect of the $Fe_3O_4$ SPION concentration was investigated. Higher concentrations led to a significant $\Delta T_2$, but an excess concentration is an obvious waste of $Fe_3O_4$ SPIONs. As shown in Fig. S2, the different $Fe_3O_4$ SPION concentrations apparently influenced the signal. The $\Delta T_2$ was recorded along with the increasing $Fe_3O_4$ SPION concentrations from 0.1 to 1.0 mg $mL^{-1}$ and reached a platform at 1.0 mg $mL^{-1}$. To ensure the completeness of the reaction, we chose 1 mg $mL^{-1}$ as the optimum $Fe_3O_4$ SPION concentration.

The concentration of S-A and S-B also influenced the hydrogel. The influence of the DNA concentration was also investigated. In Fig. S3, it is easy to see that $\Delta T/T_0$ increased before 5 μmol $L^{-1}$, but the signal change declined when the concentration was higher than 5 μmol $L^{-1}$. Therefore, the optical concentration was 5 μmol $L^{-1}$ which was diluted to 2.5 μmol $L^{-1}$ with a 1.5% Acr-Bis buffer solution.

## Analytical performance

To obtain the sensitivity of the proposed method, different concentrations of BPA were added to measure the change in the $T_2$ relaxation time. The dependence of the BPA concentration on the $T_2$ relaxation time is plotted. The results in Fig. 4a revealed that higher BPA concentrations resulted in lower $T_2$ relaxation times and higher $\Delta T_2$ values. Lower BPA concentrations showed a better linear relationship with the relaxation time $T_2$ in Fig. 4b. The BPA concentration was calculated using the following equation:

**Table 2** Detecting the BPA concentrations in environmental samples (tap water and bottled water) by the LNDH biosensor

| Sample | Added BPA (mg $mL^{-1}$) | The proposed method, mean[a] ± SD (ng $mL^{-1}$) | Recovery (%) |
|---|---|---|---|
| Tap water | $10^{-1}$ | $0.93 \times 10^{-1} \pm 0.63 \times 10^{-2}$ | 93.07 |
| | $10^{-3}$ | $9.24 \times 10^{-4} \pm 6.70 \times 10^{-5}$ | 92.37 |
| | $10^{-5}$ | $9.09 \times 10^{-6} \pm 8.90 \times 10^{-7}$ | 90.87 |
| Bottled water | $10^{-1}$ | $0.93 \times 10^{-1} \pm 0.40 \times 10^{-2}$ | 93.24 |
| | $10^{-3}$ | $9.37 \times 10^{-4} \pm 4.25 \times 10^{-5}$ | 93.73 |
| | $10^{-5}$ | $8.79 \times 10^{-6} \pm 4.76 \times 10^{-7}$ | 87.85 |

[a] Mean of three determinations

*SD* standard deviation

$$y = 143.39 + 19.19x \left(R^2 = 0.9916\right) \quad (1)$$

where $y$ and $x$ represent the relaxation time $\Delta T_2$ (ms) and the BPA concentration (ng $mL^{-1}$), respectively. The determination limit was 0.07 ng $mL^{-1}$, as calculated by:

$$(\Delta + 3\zeta)/\mathrm{K} \quad (2)$$

where $\zeta$ is the standard deviation of the blank control, $K$ is the slope of the regression equation, and $\Delta T_2$ means the average background $T_2$ relaxation time. The drinking water health standard (GB5749-2006, China) regulates the maximum level of BPA at 10 ng $mL^{-1}$.

The comparison between the proposed nanoprobe and several reported determination methods is shown in Table 1. These comparisons revealed that the LOD of this proposed method is acceptable and that the developed sensor is sensitive. The comparison results clearly revealed that the determination range is relatively wider and the LOD is lower than those of most of the presented determination methods.

Yao's team [28] used the complex of triple-doped carbon quantum dots (B, N, F-CQDs) and silver nanoparticles (AgNPs) to form molecularly imprinted polymer MIP as the identification element of the target molecule, constructing an electrochemical sensor by cyclic voltammetry. The detection is realized; the results show that the synergy between B, N, F-CQD, and AgNP significantly improves the sensitivity of the electrode and achieves the amplification of the electrical signal. The linear response range of the new sensor is 2.28~11.4 ng $mL^{-1}$ and the detection limit is 2.56 ng $mL^{-1}$. Mo's team [29] developed a BPA-sensitive electrochemical sensor based on AuPd doped with carbon nanotubes and carbon nanotubes (MWCNTs) and having amplifying current signals cooperatively. MWCNTs were used as supports to improve electron transport. The linear response range of the new sensor is 41.094–4109.4 mg $mL^{-1}$ and the detection limit is 13.698 pg $mL^{-1}$. Lin [27] reported the development of a new range-extended bisphenol A (BPA) detection method using a surface-enhanced Raman scattering lateral flow analysis (SERS-LFA) binary system. The assay includes gold nanoparticles with high SERS performance and 4-aminothiophenol (4-ATP) as Raman reporter gene. The linear response range of the new sensor is 0.01–100,000 ng $mL^{-1}$ and the detection limit is 0.073 ng $mL^{-1}$.

Based on AHN-labeled aptamers and magnetic nanoparticles, a magnetically separated fluorescent aptamer sensor for high sensitivity detection of BPA was proposed. The method utilizes the characteristics of easy separation of magnetic nanoparticles to realize the separation and detection of the original substance to be detected. The linear response range of the new sensor is 0.20~8.00 ng $mL^{-1}$ and the detection limit is 0.047 ng $mL^{-1}$.

Compared with the above method, the identification method required by our proposed method is simpler and more commonly available; the detection method has better detection ability, i.e., lower detection limit and detection range. Compared with other detection methods that use magnetic particles as the detection element, our method eliminates tedious magnetic separation steps, thereby making the operation easier and the entire detection process faster. Based on the above comparison, we can see that our detection method has certain advantages.

### Selectivity

As shown in Fig. 5, only BPA had an apparent signal among these mimics. However, the samples of BP, BPB, BPC, tb-BPA, and 6F-BPA did not have apparent signal increments. This result revealed that this proposed strategy has selectivity for BPA determination.

### Practical applicability

This method was designed for BPA determination in water samples to evaluate its practical ability and reliability. The water samples (tap water and bottled water) were spiked with BPA at $10^5$,$10^3$, and 10 ng $mL^{-1}$ respectively. As seen in Table 2, the recoveries for the spiked samples ranged from 87.85 to 97.87%. These results indicated that the aptamer-functional DNA-hydrogel system could be feasibly applied to BPA determination.

## Results and discussion

An LF-NMR DNA-hydrogel nanoprobe for BPA determination was proposed in this study. It not only has the advantages of an aptamer-functional hydrogel and $Fe_3O_4$ SPIONs but also applies LF-NMR in the EDC determination field. It effectively simplified determination operation steps and decreased the loss and damage of samples by avoiding repeated magnetic separation operations. In addition, under the optimal experimental conditions, this strategy showed a good linear range from $10^{-2}$ to $10^2$ ng $mL^{-1}$ with a limit of determination calculated to be 0.07 ng $mL^{-1}$. This aptamer-functional DNA-hydrogel with the $Fe_3O_4$ SPION system was successfully applied to detect BPA in the tap water and bottled water samples and showed a good recovery (87.85~97.87%). This strategy will provide a new idea for EDC determination and broaden the application field of LF-NMR. The uniform dispersion of magnetic nanoparticles is one of the key factors affecting the stability of the detection system. Therefore, the dispersion of magnetic nanoparticles is one of the limiting factors of this method.

**Acknowledgments** This work was supported by the National Natural Science Foundation of China [grant numbers 81773482, 21477162], The National Key Research and Development Program of China [grant number 2018YFC1603500].

## Compliance with ethical standards

**Conflict of interest** The author(s) declare that they have no competing interests.

## References


1. Li MK, Hu LY, Niu CG, Huang DW, Zeng GM (2018) A magnetic separation fluorescent aptasensor for highly sensitive detection of bisphenol A. Sens Actuator B-Chem 266:805–811
2. Usman A, Ahmad M (2019) Computational study suggesting reconsideration of BPA analogues based on their endocrine disrupting potential estimated by binding affinities to nuclear receptors. Ecotoxicol Environm Safety 154-161
3. de Oliveira ML, Rocha BA, Souza VCD, Barbosa F (2019) Determination of 17 potential endocrine-disrupting chemicals in human saliva by dispersive liquid-liquid microextraction and liquid chromatography-tandem mass spectrometry. Talanta 196:271–276
4. Lim HJ, Lee E-H, Lee S-D, Yoon Y, Son A (2018) Quantitative screening for endocrine-disrupting bisphenol A in consumer and household products using NanoAptamer assay. Chemosphere 211:72–80
5. Liu Z, Li Y, Sun L, Yang H, Zheng X, Wang L (2019) Investigation of diazo-derivatization of bisphenol A and its applicability for quantitation in food safety inspections using high-performance liquid chromatography. Biomedical Chromatography 3:e4419
6. Yamazaki E, Yamashita N, Taniyasu S, Lam J, Lam PKS, Moon H-B, Jeong Y, Kannan P, Achyuthan H, Munuswamy N, Kannan K (2015) Bisphenol A and other bisphenol analogues including BPS and BPF in surface water samples from Japan, China, Korea and India. Ecotoxicology and Environmental Safety 122:565–572
7. Zhou Q, Jin Z, Li J, Wang B, Wei X, Chen J (2018) A novel air-assisted liquid-liquid microextraction based on in-situ phase separation for the HPLC determination of bisphenols migration from disposable lunch boxes to contacting water. Talanta 116-121
8. Wang X, Gao M, Zhang Z, Gu H, Liu T, Yu N, Wang X, Wang H (2018) Development of CO2-mediated switchable hydrophilicity solvent-based microextraction combined with HPLC-UV for the determination of bisphenols in foods and drinks. Food Anal Methods 8:2093–2104
9. Hao Z, Xiao Y, Jiang L, Bai W, Huang W, Yuan L (2018) Simultaneous determination of bisphenol A, bisphenol F, 4-nonylphenol, 4-n-nonylphenol, and octylphenol in grease-rich food by carb/PSA solid-phase extraction combined with high-performance liquid chromatography tandem mass spectrometry. Food Anal Methods 2:589–597
10. Zhang J, Xu X, Chen L (2018) An ultrasensitive electrochemical bisphenol A sensor based on hierarchical Ce-metal-organic framework modified with cetyltrimethylammonium bromide. Sens. Actuator B-Chem. 425-433
11. Kashefi-Kheyrabadi L, Kim J, Gwak H, Hyun K-A, Bae NH, Lee SJ, Jung H-I (2018) A microfluidic electrochemical aptasensor for enrichment and detection of bisphenol A. Biosens Bioelectron 457-463
12. Ekomo VM, Branger C, Bikanga R, Florea A-M, Istamboulie G, Calas-Blanchard C, Noguer T, Sarbu A, Brisset H (2018) Detection of bisphenol A in aqueous medium by screen printed carbon electrodes incorporating electrochemical molecularly imprinted polymers. Biosens Bioelectron 156-161
13. Ben Messaoud N, Lahcen AA, Dridi C, Amine A (2018) Ultrasound assisted magnetic imprinted polymer combined sensor based on carbon black and gold nanoparticles for selective and sensitive electrochemical detection of bisphenol A. Sens. Actuator B-Chem. 304-312
14. Abnous K, Danesh NM, Ramezani M, Alibolandi M, Taghdisi SM (2018) A novel electrochemical sensor for bisphenol A detection based on nontarget-induced extension of aptamer length and formation of a physical barrier. Biosens Bioelectron 204-208
15. Liu L, Zhou X, Ma R, He M, Shi H, Yi Q (2018) High-throughput biomolecular interaction analysis probing by an array fluorescent biosensor platform. Sens. Actuator B-Chem 259:888–893
16. Liu L, Shan D, Zhou X, Shi H, Song B, Falke F, Leinse A, Heideman R (2018) TriPleX (TM) waveguide-based fluorescence biosensor for multichannel environmental contaminants detection. Biosens Bioelectron 117-121
17. Lee E-S, Kim GB, Ryu S-H, Kim H, Yoo HH, Yoon MY, Lee J-W, Gye MC, Kim Y-P (2018) Fluorescing aptamer-gold nanosensors for enhanced sensitivity to bisphenol A. Sens. Actuator B-Chem. 371-379
18. Guan T, Sun Y, Zhang T, Li T, Li Z, Zhang Y, Zhang J, Wang Y (2018) Simultaneous determination of bisphenol A and its halogenated analogues in soil by fluorescence polarization assay. J Soils Sediments 3:845–851
19. McCracken KE, Tat T, Paz V, Yoon J-Y (2017) Smartphone-based fluorescence detection of bisphenol A from water samples. RSC Adv 15:9237–9243
20. Xue CS, Erika G, Jiri H (2019) Surface plasmon resonance biosensor for the ultrasensitive detection of bisphenol A. Anal Bioanal Chem 411:5655–5658
21. Wang Z, Yan R, Liao S, Miao Y, Zhang B, Wang F, Yang H (2018) In situ reduced silver nanoparticles embedded molecularly imprinted reusable sensor for selective and sensitive SERS detection of bisphenol A. Appl Surf Sci 323-331
22. Xianyu YL, Dong YZ, Wang ZL, Xu ZL, Huang RM, Chen YP (2019) Broad-range magnetic relaxation switching bioassays using click chemistry-mediated assembly of polystyrene beads and magnetic nanoparticles. ACS sensors 7:1942–1949
23. Wu L, Xianyu YL, Wang ZL, Dong YZ, Hu XB, Chen YP (2019) Amplified magnetic resonance sensing via enzyme-mediated click chemistry and magnetic separation. Anal Chem 24:15555–15562
24. Kirtil E, Oztop MH (2016) H-1 nuclear magnetic resonance relaxometry and magnetic resonance imaging and applications in food science and processing. Food Eng Rev 1:1–22
25. Goncalves C, Pereira P, Gama M (2010) Self-assembled hydrogel nanoparticles for drug delivery applications. Materials 2:1420–1460
26. Ischakov R, Adler-Abramovich L, Buzhansky L, Shekhter T, Gazit E (2013) Peptide-based hydrogel nanoparticles as effective drug delivery agents. Bioorg Med Chem 12:3517–3522
27. Lin L-K, Stanciu LA (2018) Bisphenol A detection using gold nanostars in a SERS improved lateral flow immunochromatographic assay. Sens. Actuator B-Chem 222-229
28. Yao J, Chen M, Li NN, Liu CH, Yang M (2019) Experimental and theoretical studies of a novel electrochemical sensor based on molecularly imprinted polymer and B, N, F-CQDs/AgNPs for enhanced specific identification and dual signal amplification in highly selective and ultra-trace bisphenol S determination in plastic products. Analytica Chimica Acta 36-48
29. Mo FY, Xie JW, Wu TT, Liu ML, Zhang YY, Yao SZ (2019) A sensitive electrochemical sensor for bisphenol A on the basis of the AuPd incorporated carboxylic multi-walled carbon nanotubes Food Chem 253-259